GALAXY MORPHOLOGICAL SEGREGATION IN CLUSTERS: LOCAL VS. GLOBAL CONDITIONS

Mariano Domínguez, Hernán Muriel and Diego G. Lambas
Grupo de Investigaciones en Astronomía Teórica y Experimental (IATE)
Observatorio Astronómico de Córdoba, Laprida 854, 5000 Córdoba, Argentina.
CONICET, Buenos Aires,Argentina.
mardom@oac.uncor.edu, hernan@oac.uncor.edu, dgl@oac.uncor.edu

ABSTRACT

We study the relative fraction of galaxy morphological types in clusters, as a function of the projected local galaxy density and different global parameters: cluster projected gas density, cluster projected total mass density , and reduced clustercentric distance. Since local and global densities are correlated, we have considered different tests to search for the parameters to which segregation show the strongest dependence. Also, we have explored the results of our analysis applied to the central regions of the clusters and their outskirts. We consider a sample of clusters of galaxies with temperature estimates to derive the projected mass density profile and the 500 density contrast radius (r_{500}) using the NFW model and the scaling relation respectively. The X-ray surface brightness profiles are used to obtain the projected gas density assuming the hydrostatic equilibrium model. Our results suggest that the morphological segregation in clusters is controlled by the local galaxy density in the outskirts. On the other hand, the global projected mass density, shows the strongest correlation with the fraction of morphological types in the central high density region, with a marginal dependence on the local galaxy density.

Subject headings: galaxies: clusters: general — galaxies: evolution — galaxies: fundamental parameters — intergalactic medium — X-rays

1. INTRODUCTION

The difference between the population of galaxies in the field and in clusters is well known since the early 1930s. Oemler (1974) analyzed the proportion of elliptical, S0 and spiral galaxies and defined three different types of clusters: spiral rich, spiral poor and cD clusters. Melnick and Sargent (1977) showed that the inner region of clusters are typically populated by ellipticals and spirals are predominating in the outer regions (the well known morphological segregation, MS).

In a classic work, Dressler 1980b analyzed a sample of 55 nearby clusters finding a correlation between the fraction of different morphological types T and the local projected galaxy density Σ (hereafter T-Σ relation). Dressler concludes that galaxy morphology is a function of the local clustering rather than global conditions related to the cluster environment.

Samromà and Salvador Sole (1990) have consider a test to explore the nature of the morphological segregation. Using Dressler's data, artificial clusters were generated by randomly repositioning the polar coordinates of galaxy members around the center of the clusters. In this way any subclustering present is erased maintaining the radial clustercentric distance of each galaxy so that the global cluster properties are conserved. The T-Σ relation is analyzed for the randomized galaxies in the clusters and compared to the results for the real galaxy positions. The results of these tests are indistinguishable indicating that the T-Σ relation is controlled by global conditions rather than local subclustering.

Whitmore et al. (1991,1993, hereafter WGJ) reexamined Dressler's sample of galaxies in clusters and suggested that the morphology-clustercentric distance relation is more fundamental than the morphology-local galaxy density relation. These authors use the clustercentric normalized distance as the independent parameter, and compare the morphological fractions at the same normalized clustercentric radii but with different values of the local galaxy density. WGJ use a "characteristic radius", r_{opt}, as the radius at which the cumulative projected galaxy density falls bellow 20 galaxies Mpc^{-2}. These authors find that for small radii (about 0.5 Mpc) the elliptical fraction rise rapidly. On the other hand, the spiral fraction is essentially zero at the cluster center. WGJ interpret these results as an indication that cluster center conditions play a key role in determining galaxy morphologies in clusters and suggest that a destructive rather than a formation mechanism may be controlling their relative fractions.

The question whether local galaxy density or radial distance from the cluster center is best correlated with morphological types is still open. Dressler et al. (1997) reanalyzed the morphology-density relation by dividing their sample into centrally concentrated, regular clusters; and low-concentration, irregular clusters, finding a similar T-Σ relation in both subsamples. Nevertheless, they find a significant excess of SO's and a smaller spiral fraction in the centrally concentrated clusters when compared to the low-concentration systems.

Dressler et al. (1997, hereafter D97) also analyzed a sample of 10 clusters at redshifts between 0.37 and 0.56, and derive the corresponding T-Σ relation. For these distant clusters the authors find that the fraction of S0 galaxies is 2-3 times smaller than in low-redshift clusters suggesting that S0's are generated in large numbers only after cluster virialization.

It should be recalled, however, the possible presence of systematic effects related to projection biases in the selection of clusters from two dimensional data (see for instance Valotto, Moore, and Lambas, 2001), which may cause an artificial increase of the late type fraction in distant clusters.

Several mechanisms have been proposed in order to explain the morphological segregation. Among them we can mention ram pressure stripping (Gunn and Gott 1972, Abadi et al. 1999), gas evaporation (Cowie and Songaila 1977), merging (Lavery and Henry 1988), galaxy harassment (Moore et al. 1996), tidal striping (galaxy-galaxy and from mean cluster field; Bird and Valtonen 1990), tidal shaking (galaxy-galaxy and from the mean cluster field; Miller 1988), galactic cannibalism (Ostriker and Tremaine 1975), truncated star formation (Larson et al. 1980), etc. Also, it should be considered the effects provided by the initial conditions which may also play a role in the morphological segregation. In hierarchical models of structure formation such as CDM, different scales become non-linear simultaneously, so that the initial conditions of galaxy formation in cluster and group environments may differ from the field (intergalactic medium, tidal effects, mergers, etc).

In this work we study the relative fraction of galaxy morphologies in clusters as a function of global cluster parameters (projected mass and gas density profile), and the local projected galaxy density. Our analysis is aimed to provide a better understanding of the relevance of the proposed mechanisms involved in morphological segregation (MS) in clusters given their different dependence on gas, mass and galaxy content.

The paper is organized as follows. In Section 2 we briefly review the data used for this study. In Section 3 we explore the MS as a function of different global and local parameters, and perform a simple test to compare their relative importance. Section 4 provides a discussion of the main results and some implicances for galaxy evolution in clusters. We include in Appendix A a short discussion on the corrections applied to deal with observational biases.

2. DATA

The data consists of the clusters originally analyzed by Dressler 1980a restricted to those objects with detected intracluster gas X-ray emission and determination of its mean temperature and surface brightness distribution.

Dressler 1980a survey provides morphological determination for $\sim$ 6000 galaxies in 55 nearby clusters of galaxies. From this sample we have selected a sub-sample of 22 rich clusters (see Table 1) with estimated (or measured) gas temperature and X-ray surface brightness information. From Jones and Forman (1999) analysis of Einstein X-ray images we obtain the central gas density ρ_0, the core radii r_c and the β parameter for our subsample. Temperatures are taken from different sources in the literature and as it can be seen in Table 1, our sample comprises a wide range of temperatures going from poor cluster environments ($\sim$ 1.5 keV) to massive clusters ($\sim$ 8 keV). Cluster center coordinates in Table 1 correspond to the maximum of the X-ray emission. The other parameter quoted in this table are: Column 8: cluster redshift z; column 9: cluster temperature T_X; column 10: core radius r_c; column 11: β parameter; column 12: central density ρ_0; column 13: optical core radius r_{opt}, and column 14: 500 overdensity radius r_{500}.

We have excluded clusters with peculiarities in their X-ray luminosity distribution such as double clusters consisting in two sub-structures of comparable size and luminosity, objects with a significant presence of substructure, or strong departures from sphericity.

3. METHODS AND ANALYSIS

In this section we explore the dependence of the relative fraction of galaxy morphological types in clusters as a function of the local galaxy environment, namely the projected local galaxy density as defined by Dressler 1980b, and different global parameters: cluster projected total mass density and gas density, and two different reduced clustercentric distances.

3.1. Local galaxy density

In order to assess the relevance of local processes that may affect galaxy morphology, we compute the relative fraction of galaxy morphologies as a function of the projected local galaxy density in the same way as D97. We define the local galaxy density Σ_{Gal} in the position of each galaxy in our sample, using the same procedure as D97. We compute the rectangular area that comprises the ten nearest galaxies around each object and correct for completeness in luminosity and contamination from projections using the same methods described by WGJ, and discussed in Appendix A. The results are shown in Figure 1 which show similar results than those given by Dressler et al. (1997) indicating that the results of our subsample of X-ray clusters are representative of optically selected galaxy systems. Errors bars in all figures of this paper were computed using the bootstrap resampling technique (Barrow 1984).

3.2. Projected cluster mass density

The effects of the global cluster environment on galaxy morphology requires to compute parameters that quantify the effects of the cluster as a whole at the position of each galaxy. The total mass density is an important parameter of clusters that should be considered given its relevance to the several processes (eg. cluster tidal field, etc) that could affect galaxy morphology.

Navarro et al. (1995, hereafter NFW) have proposed an analytic universal density profile of dark matter halos based on numerical simulations and analytical models assuming spherical symmetry and accretion onto an initially overdense perturbation. NFW fitting function is

(1)
$$\rho(x) = \frac{\rho_s}{x(1+x)^2}, x = r/r_{\delta_c}$$

which describes cluster mass density profiles, where

r_{δ_c} is the radius corresponding to a mean over-density δ_c. This function has the advantage that the dark matter halos can be described with a single parameter over a broad rage of halo masses. Based on numerical simulations, Evrard et al. (1996) predict that the average cluster temperature T_X strongly correlates with r_{δ_c}, and propose the following relation:

(2)
$$r_{\delta_c}(T_X) = r_{10}(\delta_c) * (T_X/10keV)$$

The normalization $r_{10}(\delta_c)$ corresponds to the radial scale of 10 keV clusters at density contrast δ_c (2.48 Mpc) and we adopt a standard overdensity parameter $\delta_c = 500$.

Bartelmann (1996) has derived the projected mass density Σ_{Mass} profile corresponding to the NFW function:

(3)
$$\Sigma_{Mass}(x) = \frac{2\rho_s r_{\delta_c}}{x^2 - 1} * f(x)$$

$$\mathrm{f}(x) = \begin{cases} 1 - \frac{2}{\sqrt{x^2-1}} arctanh\sqrt{\frac{x-1}{x+1}}, & \text{if } x > 1 \\ 1 - \frac{2}{\sqrt{1-x^2}} arctanh\sqrt{\frac{1-x}{1+x}}, & \text{if } x < 1 \\ 0, & \text{if } x = 1 \end{cases}$$

We consider the mean cluster temperatures quoted in Table 1 in equation (2) to derive R_{500}. Then the projected mass density Σ_{Mass} at the position of each galaxy can then be obtained by equation (3).

For all clusters we compute the relative fraction of morphological types in bins of Σ_{Mass}. The results are shown in Figure 2 where it can be appreciated a very significant dependence of the relative fraction of galaxy morphologies on the local mass density inferred from the projected NFW profile.

Local vs. global effects might be reflected in the different dependence of the morphological segregation on Σ_{Gal} and Σ_{Mass}. By comparison of figures 1 and 2, it can be appreciated that both Σ_{Mass} and Σ_{Gal} provide a good correlation with the relative fraction of morphological types. However, given the correlation between these two densities as shown in Figure 3, it is important to analyze whether they are primary or secondary parameters in the morphological segregation.

In order to address this point, we consider for simplicity two morphological groups: early (ellipticals + S0) and late (spirals + irregulars) types in the following tests:

(1) our galaxy sample is divided according to Σ_{Gal} for bins in Σ_{Mass}. For each bin in Σ_{Mass} we have divided our sample in three equal number sub-samples: low, intermediate and high Σ_{Gal}. For the high and low projected galaxy density sub-samples we computed the fraction of early and late types as a function of the global mass density (in the position of each object). The results of this test are displayed in figures 4a and 4b.

(2) we have divided our galaxy sample according to Σ_{Mass} for bins in Σ_{Gal}. For each bin in Σ_{Gal} we divide our sample in three equal number sub-samples: low, intermediate and high Σ_{Mass}. For the high and low projected mass density sub-samples we computed the fraction of early and late types as a function of the local galaxy density. The results of this second test are shown in figures 4c and 4d.

It should be recalled that the results shown in figures 4a and 4b show significant differences in the fraction of morphological types between the high and low Σ_{Gal} subsamples at low values of Σ_{Mass}, ie. typically in the outskirts of the clusters. On the other hand, figures 4c and 4d show significant differences in the relative fraction of early and late types between the high and low Σ_{Mass} subsamples at high values of Σ_{Gal}, ie. in the central virialized regions of clusters. In order to provide a quantitative measurement of these effects we have computed the differences of the relative fraction of morphological types for the high and low density subsamples. We sum these differences and compute the corresponding averages and dispersions across the different bins in total range of densities (see table 2, column 1).

Given the marked difference between the inner and outer regions of the clusters, we have considered the associated threshold densities: $\log(\Sigma_{Mass}) \approx -0.03$ and $\log(\Sigma_{Gal}) \approx 1.1$ (defining the Low Density and High Density samples in table 2). These values correspond on average to a mean overdensity $\delta_c = 500$, a conservative estimate of the boundary between the inner, virialized region of the clusters and their recently accreted, still settling outer envelopes as discussed by Evrard et al.(1996). The results of tests 1 and 2 can be appreciated by inspection to Table 2, where the average differences in morphological fractions, dispersions and statistical significance as well as the percentages of galaxies used in each computation are listed.

The results of tests 1 and 2 strongly suggest that local galaxy density should not be considered as the unique parameter that determines the relative fractions of galaxy morphologies in clusters of galaxies. In the outskirts of clusters (quoted as Low Density in table 2), Σ_{Gal} accounts for most of the effect while Σ_{Mass} may be considered a primary parameter in the high density virialized region of clusters.

3.3. Gas density profile

Other important global parameter worth to be considered is the intracluster gas density which may induce important morphological transformations in galaxies orbiting in the cluster potential well, such as ram pressure processes or gas evaporation.

For an isothermal gas distribution in hydrostatic equilibrium the gas density profile can be obtained by fitting the X-ray surface brightness distribution with the well known beta model:

(4)

$$I_x = I_0[1 + (r/r_c)^2]^{-3\beta+1/2}$$

Fitting β and r_c from the previous equation the gas density can be derived as follows

(5)

$$\rho_{gas} = \rho_0[1 + (r/r_c)^2]^{-3\beta/2}$$

This equation can be projected in order to derive the projected intracluster gas density (Abadi and Navarro private communication):

(6)

$$\Sigma_{Gas}(r) = \rho_0 r_c[1 + (r/r_c)^2]^{(1-3\beta_f)/2} B(1/2, \frac{3\beta_f - 1}{2})$$

where

$$B(x, y) = \frac{\Gamma(x)\Gamma(y)}{\Gamma(x + y)}$$

We have computed the fraction of galaxies by morphological types as a function of the Σ_{Gas} for our sample. The results of this correlation are displayed in Figure 5.

We have applied similar tests as those described in the previous section with Σ_{Gas} and Σ_{Gal} so that now we divide our galaxy sample according to Σ_{Gal} for bins in Σ_{Gas} and for each bin in (Σ_{Gas}) we consider three equal number sub-samples: low, intermediate and high (Σ_{Gal}) and compute the fraction of morphological types of galaxies as a function of the projected gas density for the high and low galaxy density subsamples (test 3). In a similar way we perform the complementary test for bins in Σ_{Gal} and subsamples in Σ_{Gas} (test 4).

The results of these tests are displayed in figure 6 and are also summarized in table 2.

By inspection to the results of mass and gas projected profiles (figures 4 and 6, and table 2) vs. the local galaxy density we can infer that the relative fraction of galaxy morphology shows a stronger correlation with the NFW profile in comparison to the β model profile.

3.4. Dependence on clustercentric distances normalized to r_{opt} and r_{500}

A usually adopted way to analyze the dependence of galaxy morphology on global cluster parameter is to compute galaxy clustercentric distances normalized to a cluster characteristic radius.

WGJ have re-examined the relative fraction of galaxy morphological types in Dressler's sample of clusters concluding that the clustercentric radial distance is a primary parameter in contrast to the local galaxy density, a secondary parameter in the morphology segregation. We have applied similar tests to those described in the previous sections and for this case, our analysis is equivalent to that in WGJ.

We divide our galaxy sample according to Σ_{Gal} for bins in r/r_{opt} and for each bin in r/r_{opt} we consider three equal number sub-samples: low, intermediate and high Σ_{Gal} and compute the fraction of morphological types as a function of r/r_{opt} for the high and low local galaxy density sub-samples (test 5). In a similar way we perform the complementary test for bins in Σ_{gal} and subsamples in high and low normalized radial distance (test 6).

The results of these tests are shown in Figure 7 and displayed in Table 2. It can be seen that neither Σ_{Gal} nor r/r_{opt} can be considered as a primary parameter defining the relation between galaxy morphology and environment. The conclusion from a similar analysis by WGJ applied to the very central regions (within $r/R_{opt} = 0.25, \simeq 0.15 Mpc$ on average for our sample) is that a normalized clustercentric distance r/r_{opt} acts as a single parameter driving the galaxy morphological segregation. This is consistent with our results in the first two bins of figure 7a and 7b which correspond to these scales. By inspection to these figures, it can also be appreciated the significant dependence of the relative fraction of galaxy morphologies on Σ_{gal} at larger distances from the cluster centers.

Several works use r_{200} or r_{500} as a characteristic cluster radius (see for instance Yee et al. 1996) in order to make a proper comparison of different clusters. In this subsection we adopt the r_{500} radius to normalize each galaxy radial distance and we apply similar tests as those described previously. The results of the corresponding tests 7 and 8 are displayed in figure 8 (see also Table 2). By inspection to these figures and Table 2 we conclude that the dependence of galaxy morphology relative fractions on r/r_{500} is similar to that obtained with r/r_{opt}. Nevertheless, we find these dependencies considerably less significant than that on the NFW projected mass density profile as it can be seen by comparison of figures 4 and 8.

3.5. Morphological segregation in clusters with low / high X-ray luminosity and intracluster gas temperature

Different authors have analyze possible dependencies of the morphological segregation on the X-ray luminosity. Dressler 1980b computed the T-Σ relationship for eight strong X-ray emitters ($L_x \geq 10^{44} ergs^{-1}$) finding similar relations between morphological types and galaxy density than in the total sample. WGJ divided a sample of 39 clusters with X-ray luminosity in three sub-samples finding no significant dependence of the morphological fractions as a function of clustercentric radius on the cluster X-ray luminosity. For our sample X-ray luminosities and intracluster gas temperatures are available for all clusters. In order to explore the correlations between the fraction of morphological types and the global and local parameters in different cluster environments we have divided our sample into high and low cluster temperature and luminosity subsamples. In a similar way as done in the previous sections, we computed the fraction of spiral galaxies for high and low Σ_{Mass} and Σ_{Gal} values in bins of Σ_{Gal} and Σ_{Mass} respectively, for two subsamples of clusters, luminous ($L_X \geq 1.638 \cdot 10^{44} erg.s^{-1}$) and non luminous ($L_X \leq 1.123 \cdot 10^{44} erg.s^{-1}$). We have also applied the same analysis to the two subsamples defined by hot ($T_X \geq 3.7keV.$), and cold ($T_X \leq 3.4keV.$) clusters. The results of these tests show a lack of a strong dependence on luminosity and temperature, in agreement with Dressler 1980b and WGJ. However, in the central regions of the subsample of high temperature and X-ray luminosity clusters we notice a stronger dependence of the relative morphological fractions on the global mass density vs. the local galaxy density when compared to low temperature/X-ray luminosity cluster subsample.

4. DISCUSSION AND CONCLUSIONS

In hierarchical scenarios for structure formation in the universe, clusters are assembled from smaller subunits, so that the local galaxy density, associated to these primordial clumps, could play a significant role in the segregation of morphological types. On the other hand, the several mechanisms related to galaxy evolution within the potential well of clusters (RAM pressure, tidal effects, etc.) could also explain the morphological segregation and its relation to global parameters.

The results of our analysis suggests that there are different mechanisms controlling the morphological segregation depending on the galaxy environment. We find that mechanisms of global nature dominate in high density environments, namely, the virialized region of clusters, while local galaxy density as defined by Dressler 1980b is the relevant parameter in the outskirts where the influence of the cluster as a whole is relatively small compared to local effects.

As it can be inferred by inspection to figure 4, a primary parameter in the segregation of morphological types in high density regions is the global cluster mass density at the position of the galaxies, computed using the scaling relationship between the mean cluster temperature and the projected NFW mass density profile. We find that the relative fraction of galaxy morphologies shows a stronger dependence on the local NFW projected density profile compared to other radial distances normalizations such as r_{500} or r_{opt}. Therefore, these results might be applied to other studies of galaxy properties in clusters such as star formation rate, fraction of blue galaxies, etc. that show a significant dependence on radial distance to the cluster centers.

By comparison of the results corresponding to the NFW and the β model profiles (projected mass and gas density respectively) we conclude that the relative fraction of galaxy morphologies is more strongly correlated with the NFW profile. This result may serve to assess the importance of tidal effects and gaseous phenomena operating in the transformation of spiral galaxies into S0s.

Our results give support to the idea that tidal force effects produced by the cluster potential, galaxy harassment, or truncated star formation among others physical mechanisms would be primary in driving the observed morphological segregation in clusters of galaxies.

We have also taken into account different cluster properties in our analysis by considering subsamples of high/low cluster temperature and high/low X-ray luminosity. The results of these analysis are similar to those obtained for the total sample although in the high density regions of hot clusters we find a tendency of a stronger morphological segregation as a function of Σ_{Mass}.

5. Appendix: Corrections for background / foreground galaxies and magnitude cutoff.

As is was extensively discussed by WGJ, corrections due to background/foreground galaxies are to be applied when dealing with relative morphological fractions in clusters. For those computations requiring estimates of the local galaxy density we have applied corrections in the same way as WGJ. We recall that the total mass density profile is obtained from the mean cluster temperatures of the intracluster gas, estimates which are nearly free of projection effects.

However, estimates of the relative fraction of galaxy morphological types will be biased when a background/foreground galaxy is taken as a center to compute the corresponding gas/mass density. To correct for this effect we have take into account the correlation between galaxy projected density and the percentage of background/foreground galaxies given by WGJ. We estimate the corrections assuming a correlation between mass/gas density and the local galaxy density (see Figure 3 which is a good approximation given the small difference of observed and actual relative fraction of morphological types due to projection effects. Using the correlation found by WGJ between absolute magnitude and cumulative number of galaxies by morphological types we have also corrected for absolute magnitude cutoff. This effect takes into account the fact that clusters are at different distances with the same limiting apparent magnitude.

Acknowledgments

This work was partially supported by the Consejo de Investigaciones Científicas y Técnicas de la Republica Argentina, CONICET, the Consejo de Investigaciones Científicas y Tecnológicas de la Provincia de Córdoba, CONICOR, and Fundación Antorchas, Argentina. We thank the Referee for helpful suggestions.

REFERENCES

Abadi, M. G., Moore, B., and Bower, R. G. 1999, MNRAS 308, 947.

Barrow, J. D., Sonoda, D. H., Bhavsar, S. P. 1984, MNRAS 210, 19.

Bartelmann, M., 1996 Astron. Astrphys. 313, 697.

Byrd, G., and Valtonene, M., 1990 ApJ. 350, 89.

Cowie,L. L., and Songaila,A. 1977 Nature 266, 501.

Dressler, A. 1980a, ApJS. 424,565.

Dressler, A. 1980b, ApJ. 236, 351.

Dressler, A., Oemler, A. Jr., Cousch, W. J., Smail, I., Ellis, R. S., Barger, A., Butcher, H., Poggianti, B. M., and Sharples, R. M. 1997, ApJ. 490, 577 (D97).

Evrard A. E. , Metzler, C. A., and Navarro, J. F. 1996 ApJ. 469, 494.

Gunn, J. E., and Gott, J. R. 1972, ApJ. 176, 1.

Jones, C., and Forman, W. 1999 ApJ. 511,.65.

Lavery, R. J., and Henry, P. J. 1988, ApJ 330, 596.

Larson, R. B., Tinsley, B. M., and Caldwell, c. n. 1980 ApJ. 237, 692.

Melnick, J., and Sargent, W. L.1997, ApJ. 215, 401.

Miller, R. H., 1988 Comments on Ap. 13, 1.

Moore, B.,Katz, N., Lake, G., Dresssler, A., and Oemler, A., 1996 Nature 379, 613.

Navarro, J. F., Frenck, C. S., and White, S. D. M. 1995 MNRAS 275, 720 (NFW).

Oemler A. Jr. 1974, ApJ. 194, 1.

Ostriker, J. P., and Tremaine, S. D., 1975 ApJ (letters) 202, L113.

Samromà, M., and Salvador-Sole, E., 1990, ApJ. 360, 16.

Valotto, C., Moore, B., and Lambas, D. 2001, ApJ, in press.

Whitmore, B. C., and Gilmore, D. M. 1991, ApJ. 367, 64.

Whitmore, B. C., Gilmore, D. M., and Jones, C. 1993, ApJ. 407, 489 (WGJ).

This 2-column preprint was prepared with the AAS LaTeX macros v4.0.

Table 1

Cluster Sample.

Name	RA [1950]			Dec. [1950]			z	T_x keV	r_c Mpc	β	ρ_0 10^{-3}cm^{-3}	r_{opt} Mpc	r_{500} Mpc
A0076	00	37	25.1	+06	33	32	0.0416	1.5	0.41	0.60	0.522	0.23	0.90
A0119	00	53	43.5	-01	31	28	0.0440	5.9	0.32	0.53	1.221	0.83	1.79
A0154	01	08	22.2	+17	23	37	0.0658	3.1	0.17	0.55	1.690	0.80	1.25
A0194	01	23	20.0	-01	38	12	0.0178	1.4	0.20	0.60	0.719	0.38	0.90
A0376	02	42	57.3	+36	41	52	0.0488	5.1	0.08	0.46	3.941	1.05	1.65
A0400	02	55	00.0	+05	48	25	0.0232	2.5	0.26	0.65	4.430	0.43	1.20
A0496	04	31	20.4	-13	21	48	0.0320	3.9	0.14	0.59	5.283	0.39	1.48
A0539	05	13	55.2	+06	23	16	0.0205	3.0	0.11	0.60	3.054	0.56	1.32
A0592	07	39	56.5	+09	29	30	0.0624	3.2	0.14	0.60	2.606	0.26	1.28
A0957	10	11	07.9	-00	40	53	0.0440	2.8	0.14	0.52	1.720	0.56	1.23
A1142	10	58	17.7	+10	47	40	0.0353	3.7	0.19	0.60	0.786	0.28	1.43
A1185	11	08	03.0	+28	59	04	0.0304	3.9	0.15	0.62	1.445	0.39	1.48
A1377	11	44	40.6	+55	59	40	0.0509	2.7	0.29	0.60	0.793	0.42	1.20
A1656	12	57	18.3	+28	12	22	0.0235	8.1	0.43	0.67	2.275	1.24	2.16
A1913	14	24	25.5	+16	53	40	0.0533	2.9	0.57	0.60	0.396	0.61	1.24
A1983	14	50	36.8	+16	55	02	0.0458	2.2	0.08	0.60	3.838	0.60	1.09
A1991	14	52	13.4	+18	50	56	0.0586	5.4	0.06	0.56	10.810	0.25	1.67
A2040	15	10	21.0	+07	37	06	0.0456	2.5	0.14	0.60	1.782	0.48	1.16
A2256	17	06	44.3	+78	42	46	0.0601	7.5	0.58	0.76	1.278	1.05	1.97
A2634	23	35	54.9	+26	44	19	0.0312	3.4	0.42	0.60	0.597	0.98	1.38
A2657	23	42	22.9	+08	54	15	0.0414	3.4	0.14	0.52	3.018	0.73	1.36
Cent.	12	46	03.4	-41	02	26	0.0107	3.9	0.15	0.45	1.939	—	1.52

Table 2
Results

	Total	Outskirts	Inner
Test 1	0.12 $\pm$ 0.03 [4.6]	0.20 $\pm$ 0.06 [3.3] 37%	0.07 $\pm$ 0.02 [3.1] 63%
Test 2	0.09 $\pm$ 0.03 [3.0]	-0.01 $\pm$ 0.07 [0.2] 40%	0.16 $\pm$ 0.03 [5.3] 60%
Test 3	0.12 $\pm$ 0.03 [4.4]	0.07 $\pm$ 0.04 [1.9] 37%	0.13 $\pm$ 0.03 [4.8] 63%
Test 4	0.06 $\pm$ 0.03 [2.0]	-0.01 $\pm$ 0.07 [0.1] 49%	0.11 $\pm$ 0.03 [5.1] 51%
Test 5	0.16 $\pm$ 0.04 [4.3]	0.24 $\pm$ 0.07 [3.2] 41%	0.10 $\pm$ 0.03 [2.9] 59%
Test 6	-0.09 $\pm$ 0.03 [3.0]	-0.10 $\pm$ 0.07 [1.4] 47%	-0.08 $\pm$ 0.02 [3.4] 53%
Test 7	0.12 $\pm$ 0.03 [4.0]	0.13 $\pm$ 0.06 [2.1] 45%	0.10 $\pm$ 0.03 [3.1] 55%
Test 8	-0.04 $\pm$ 0.03 [1.0]	0.03 $\pm$ 0.08 [0.4] 42%	-0.08 $\pm$ 0.03 [2.6] 58%

Fig. 1.— Figure 1. Relative fraction of E (solid line), S0 (dotted line) and S+I (dashed line) as a function of the local galaxy density.

Fig. 2.— Figure 2. Relative fraction of E, S0 and S+I as a function of the projected mass density. Line types are the same as in figure 1.

Fig. 3.— Figure 3. Correlation between local galaxy density Σ_{Gal} and projected cluster mass density Σ_{Gas} at the position of each galaxy of the cluster sample. The solid line correspond to the best power-law fit.

Fig. 4.— Figure 4. Relative fraction of galaxy morphological types as a function of the global projected mass density Σ_{Mass} and local galaxy density Σ_{Gal}. a) Fraction of E+S0 vs. Σ_{Mass} at high (solid line), and low (dashed line) Σ_{Gal}. b) Same as 4a for the relative fraction of S+I. c) Fraction of E+S0 vs. Σ_{Gal} at high (solid line), and low (dashed line) Σ_{Mass}. d) Same as 4c for the relative fraction of S+I.

Fig. 5.— Figure 5. Relative fraction of E, S0 and S+I as a function of the projected gas density. Line types are the same as in figure 1.

Fig. 6.— Figure 6. Relative fraction of galaxy morphological types as a function of the global projected gas density Σ_{Gas} and local galaxy density Σ_{Gal}. a) Fraction of E+S0 vs. Σ_{Gas} at high (solid line), and low (dashed line) Σ_{Gal}. b) Same as 6a for the relative fraction of S+I. c) Fraction of E+S0 vs. Σ_{Gal} at high (solid line), and low (dashed line) Σ_{Gas}. d) Same as 6c for the relative fraction of S+I.

Fig. 7.— Figure 7. Relative fraction of galaxy morphological types as a function of the clustercentric projected radial distance normalized to r_{opt} and local galaxy density Σ_{Gal}. a) Fraction of E+S0 vs. r/r_{opt} at high (solid line), and low (dashed line) Σ_{Gal}. b) Same as 7a for the relative fraction of S+I. c) Fraction of E+S0 vs. Σ_{Gal} at high (solid line), and low (dashed line) r/r_{opt}. d) Same as 7c for the relative fraction of S+I.

Fig. 8.— Figure 8. Relative fraction of galaxy morphological types as a function of the clustercentric projected radial distance normalized to r_{500} and local galaxy density Σ_{Gal}. a) Fraction of E+S0 vs. r/r_{500} at high (solid line), and low (dashed line) Σ_{Gal}. b) Same as 8a for the relative fraction of S+I. c) Fraction of E+S0 vs. Σ_{Gal} at high (solid line), and low (dashed line) r/r_{500}. d) Same as 8c for the relative fraction of S+I.

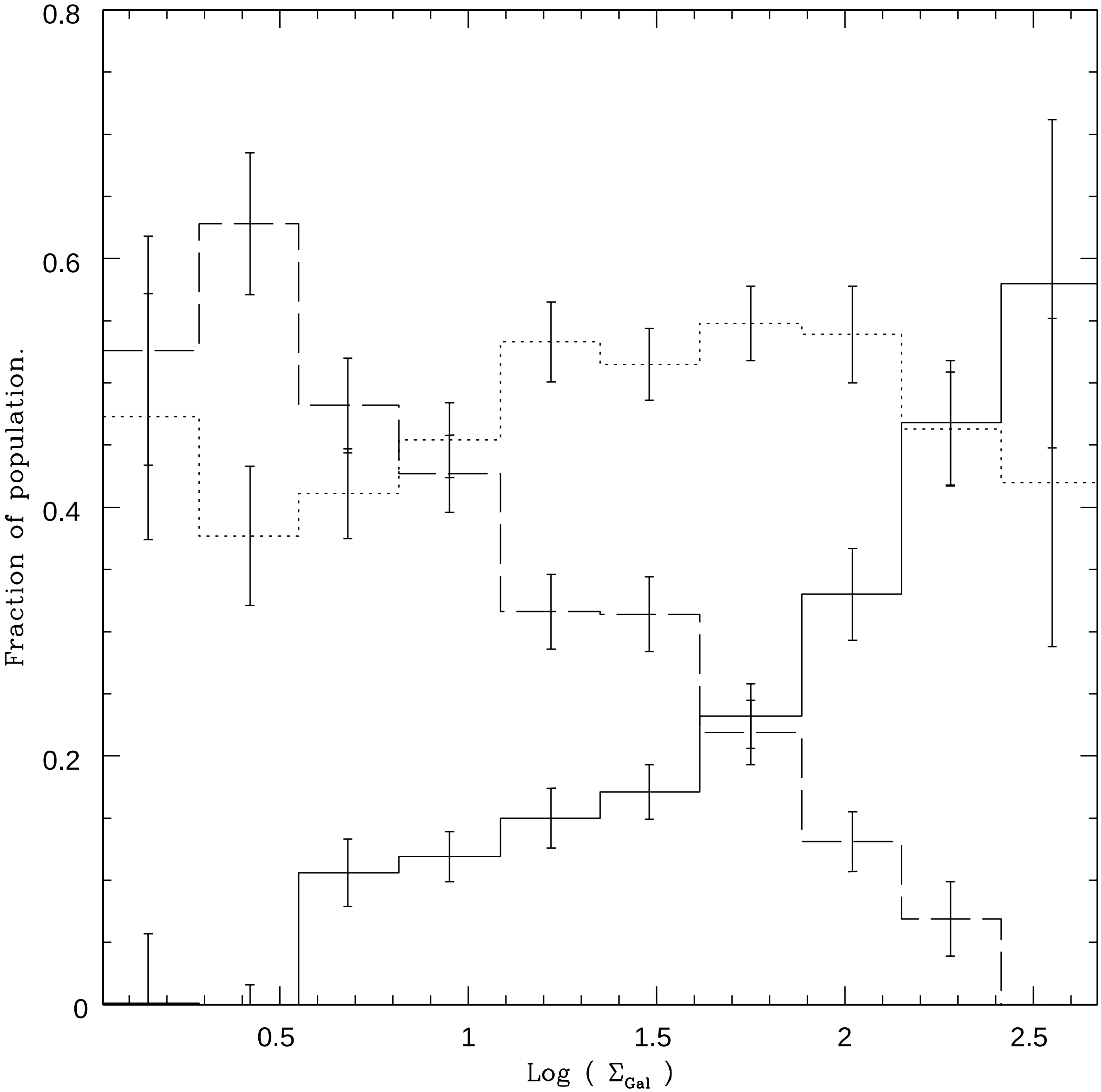

0.8
0.6
0.4
0.2
0
0.5
1
1.5
2
2.5
Fraction of population.
Log (Σ_{Gal})

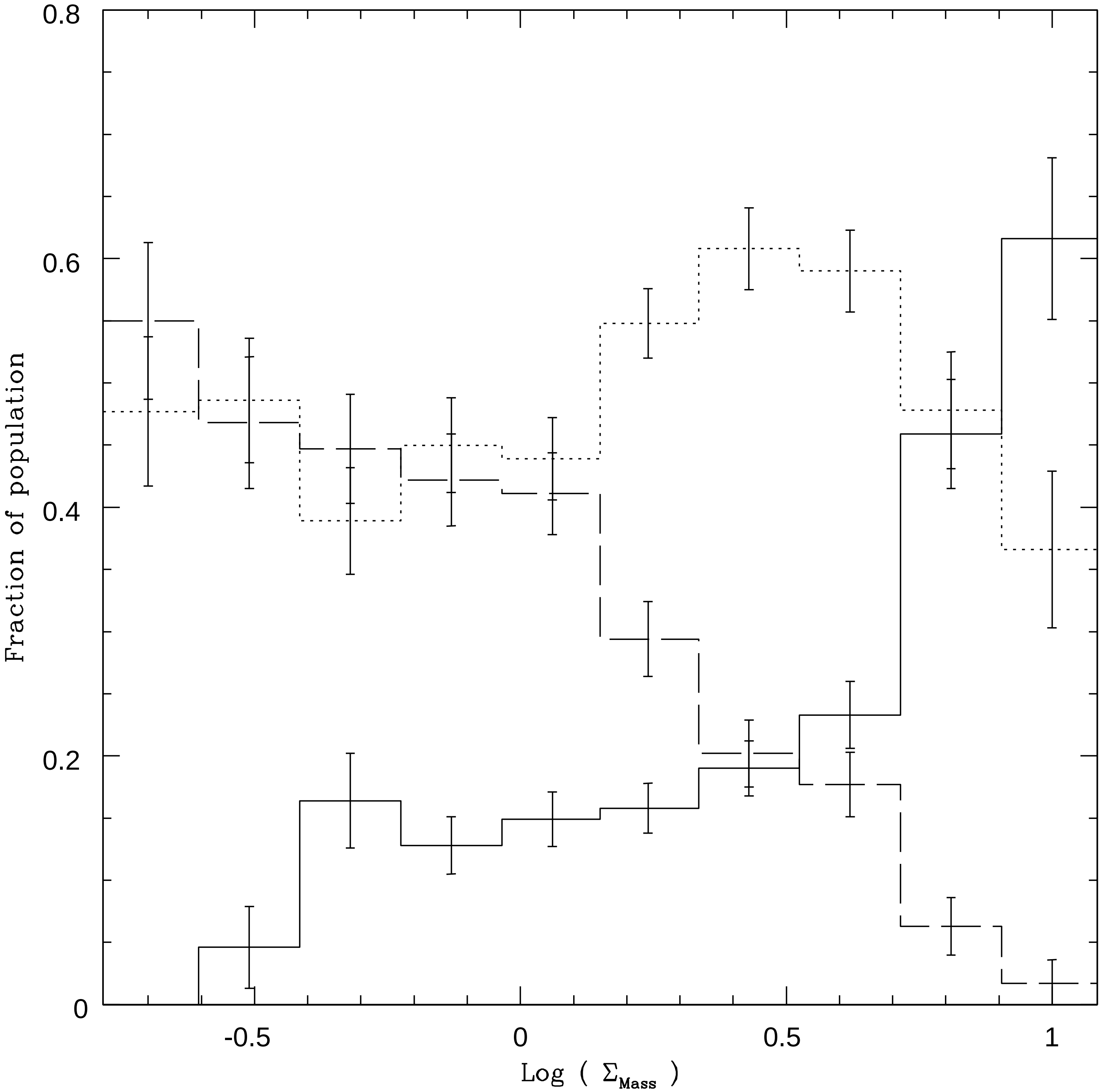
0.8
0.6
0.4
0.2
0
-0.5
0
0.5
1
Fraction of population
Log (Σ_{Mass})

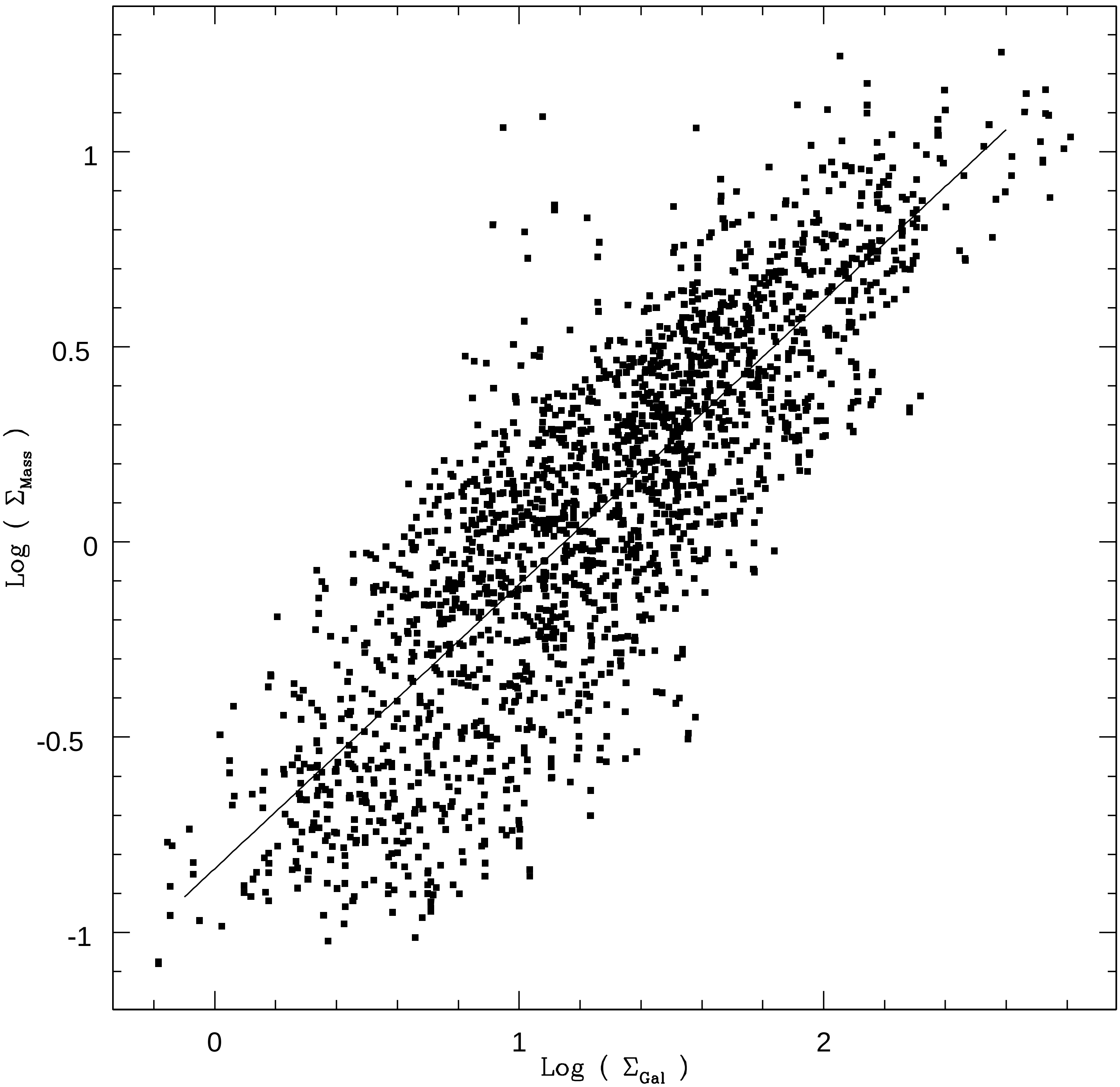

1
0.5
0
-0.5
-1
Log (Σ_{Mass})
0
1
2
Log (Σ_{Gal})

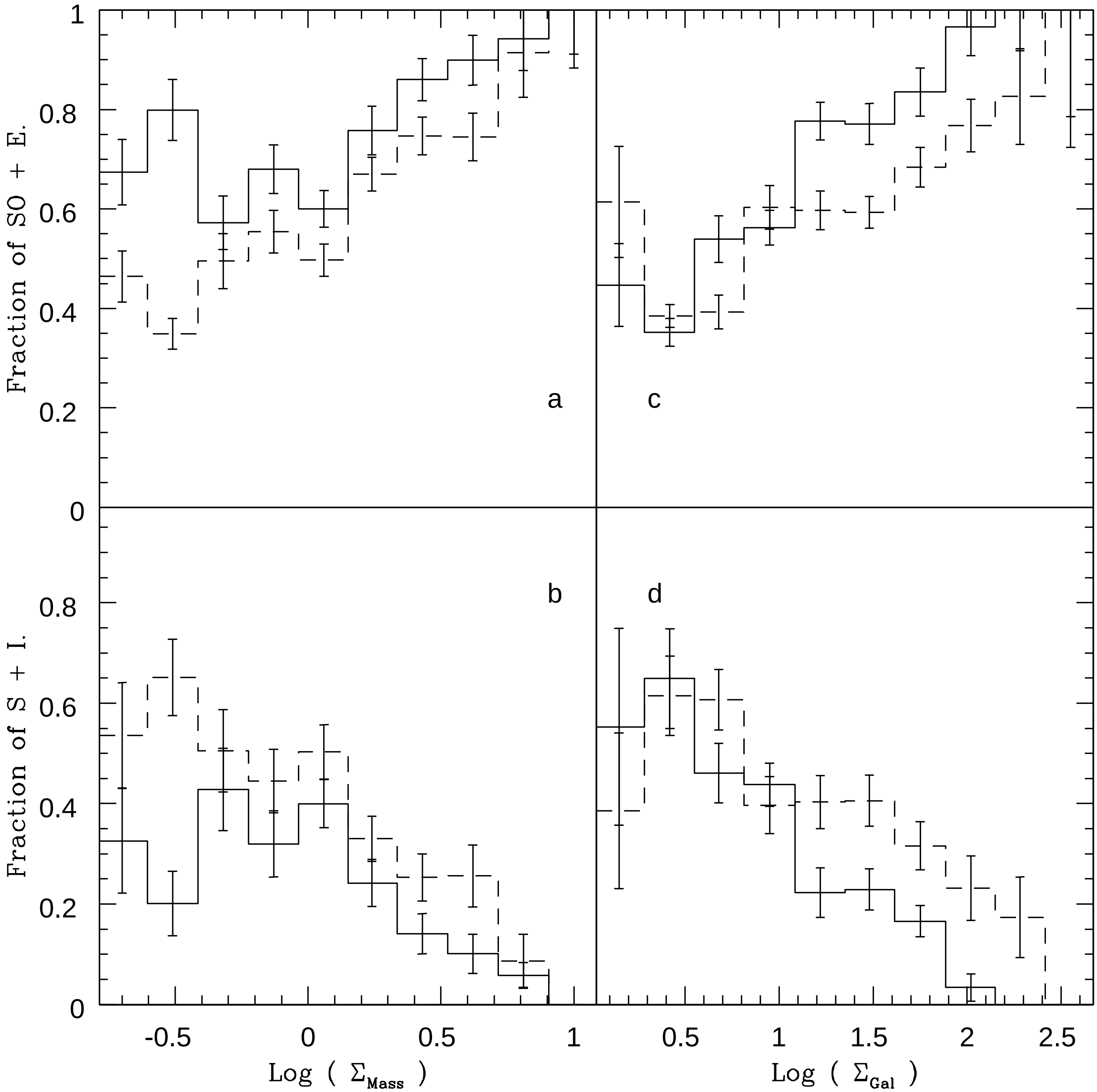

Fraction of SO + E.
Fraction of S + I.
a
b
c
d
Log (Σ_{Mass})
Log (Σ_{Gal})

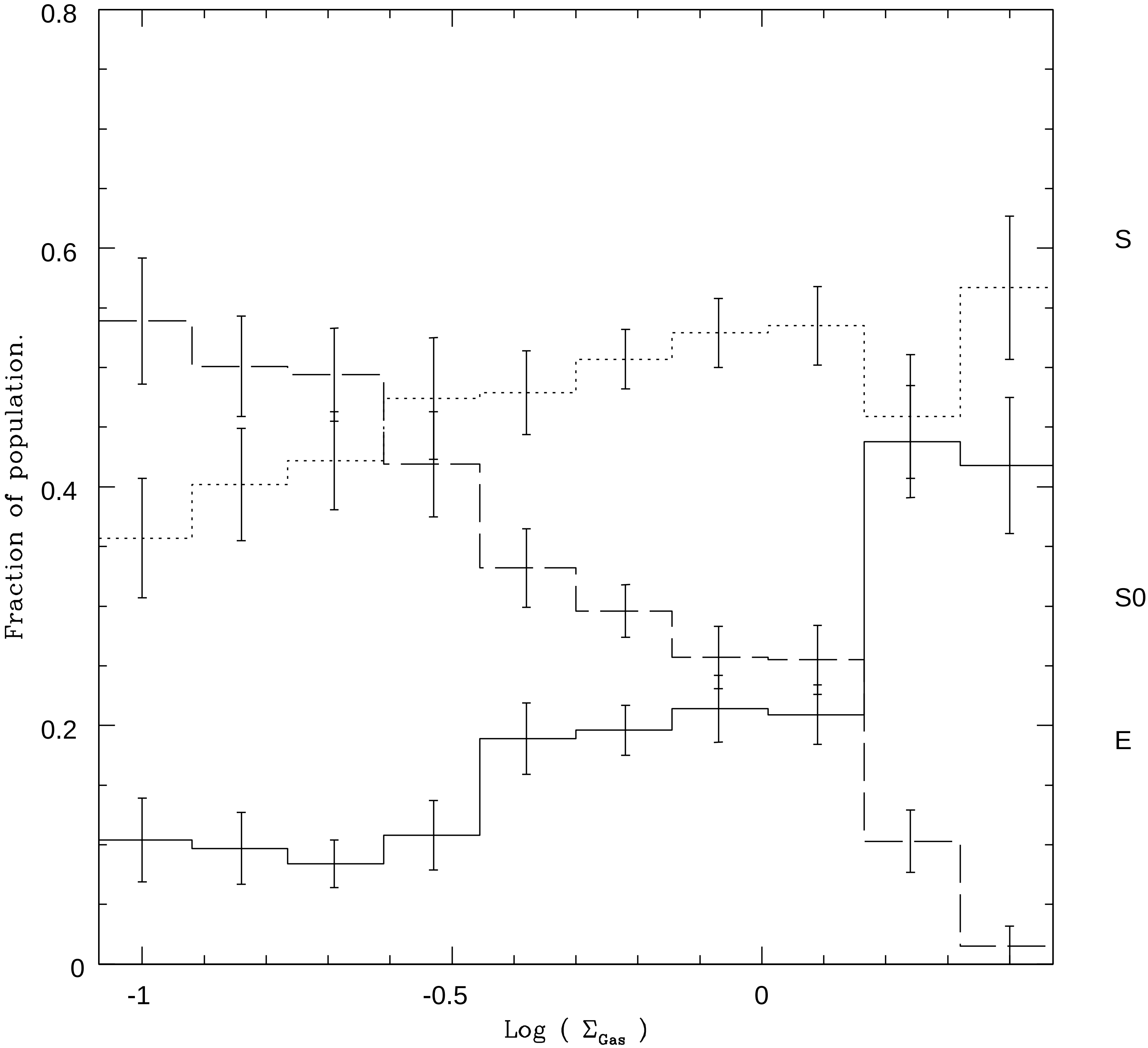

0.8
0.6
0.4
0.2
0
-1
-0.5
0
Fraction of population.
Log (Σ_{Gas})
S
S0
E

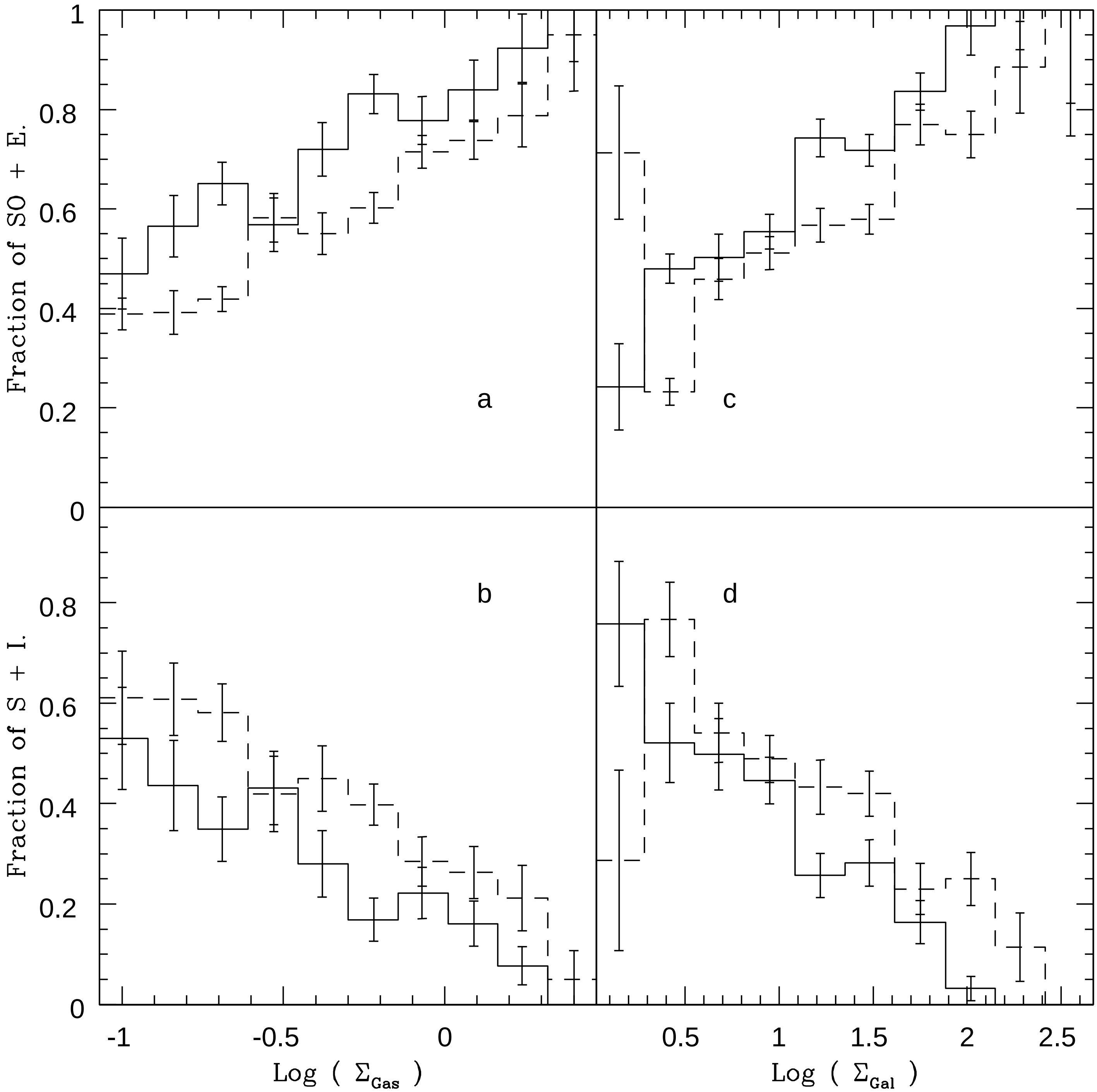

Fraction of SO + E.
Fraction of S + I.
a
b
c
d
1
0.8
0.6
0.4
0.2
0
-1
-0.5
0
0.5
1
1.5
2
2.5
Log (Σ_{Gas})
Log (Σ_{Gal})

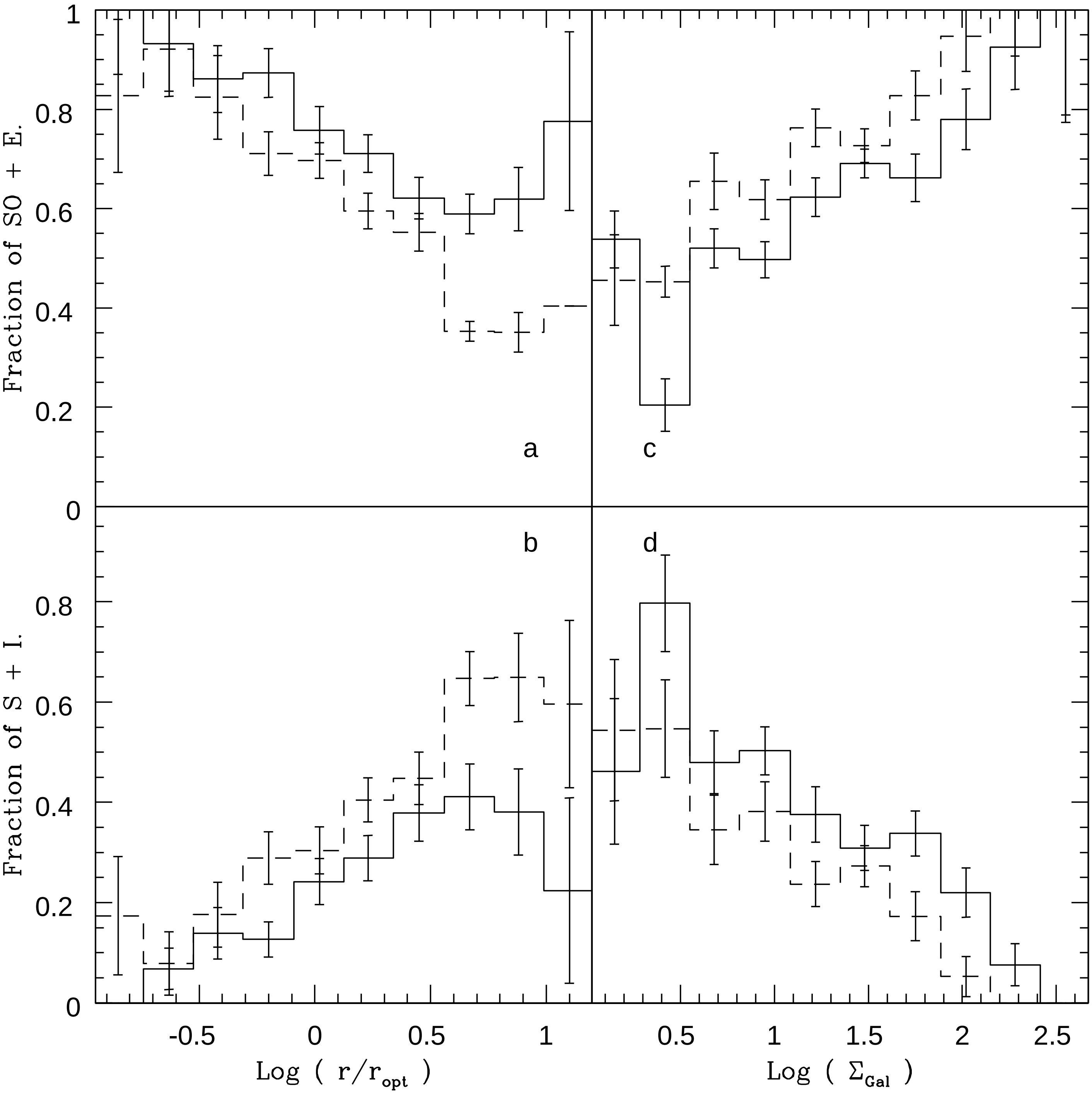

Fraction of S0 + E.
Fraction of S + I.
a
b
c
d
Log (r/r_{opt})
Log (Σ_{Gal})

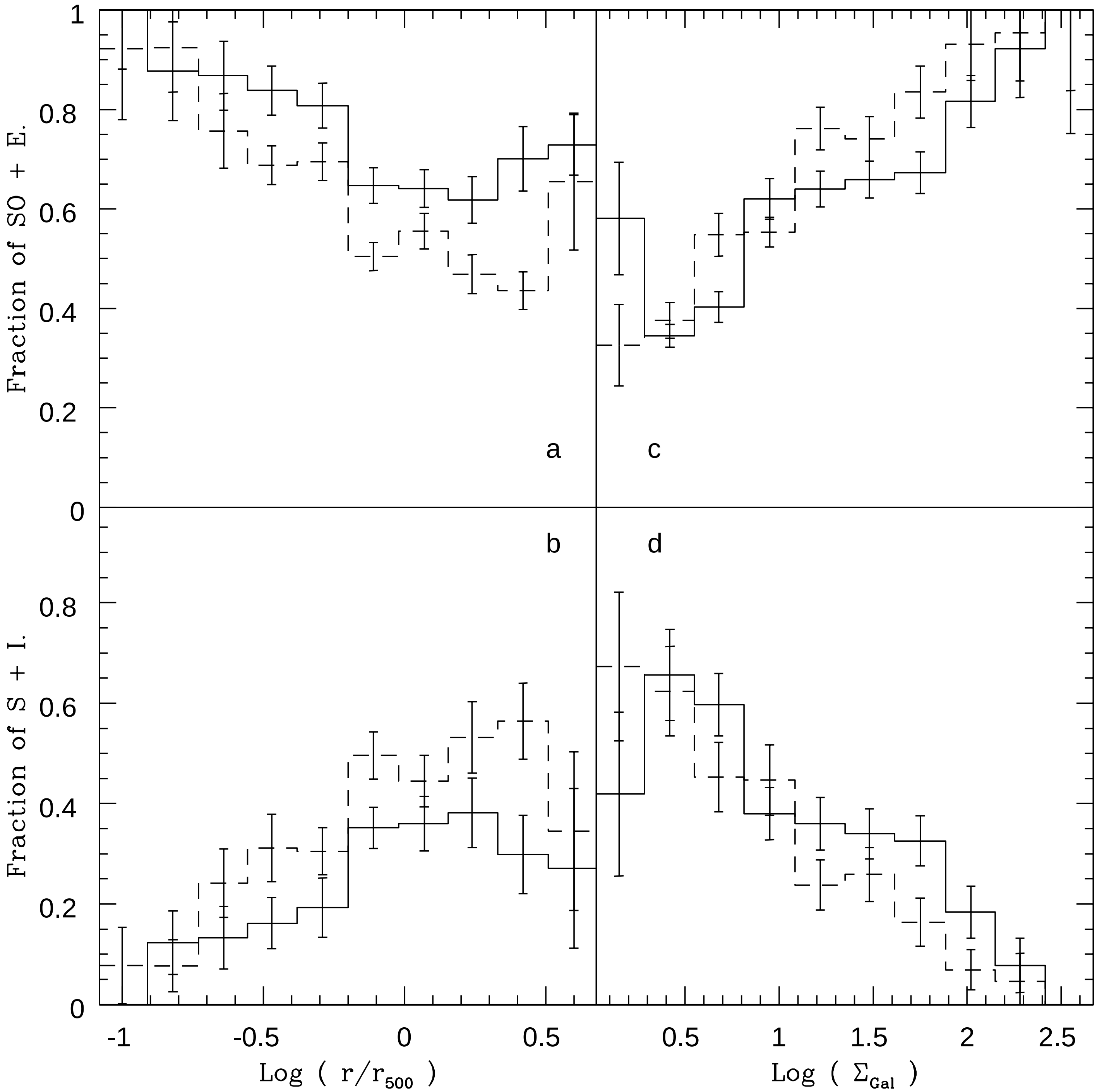

Fraction of S0 + E.
Fraction of S + I.
a
b
c
d
0
0.2
0.4
0.6
0.8
1
-1
-0.5
0
0.5
1
1.5
2
2.5
Log (r/r500)
Log (ΣGal)